

# Three asymmetric Salamo-type copper(II) and cobalt(II) complexes: Syntheses, structures and fluorescent properties



Yin-Juan Dong, Xiu-Yan Dong, Wen-Kui Dong\*, Yang Zhang, Li-Sha Zhang

School of Chemical and Biological Engineering, Lanzhou Jiaotong University, Lanzhou 730070, PR China

## ARTICLE INFO

### Article history:

Received 11 October 2016

Accepted 7 December 2016

Available online 18 December 2016

### Keywords:

Asymmetric Salamo-type ligand  
Complex  
Synthesis  
Crystal structure  
Fluorescence property

## ABSTRACT

Three new supramolecular complexes,  $[\text{Cu}(\text{HL}^1)]$  (**1**),  $[\text{Cu}(\text{L}^2)\text{H}_2\text{O}]$  (**2**) and  $[\text{Co}_2(\text{L}^2)_2]\cdot 3\text{CH}_3\text{CN}$  (**3**), were designed and synthesized by the reaction of 5-hydroxy-4',6'-dibromo-2,2'-[ethylenediylidioxibis(nitrilomethylidyne)]diphenol ( $\text{H}_3\text{L}^1$ ) with Cu(II) acetate hydrate (for **1**); and 6-methoxy-4',6'-dibromo-2,2'-[ethylenediylidioxibis(nitrilomethylidyne)]diphenol ( $\text{H}_2\text{L}^2$ ) with Cu(II) acetate hydrate (for **2**) and cobalt(II) acetate tetrahydrate (for **3**), respectively, and were characterized by element analyses, X-ray crystallography, FT-IR, UV-Vis and fluorescence spectra. Complex **1** is mononuclear and tetra-coordinated and adopts a distorted square-planar geometry, likewise, complex **2** is mononuclear and penta-coordinated with a square-pyramidal geometry, however, complex **3** is dinuclear with the two Co(II) atoms having the same coordination environments and adopt a trigonal bipyramidal geometry. These self-assembling complexes form different dimensional supramolecular structures through inter- and intramolecular hydrogen bonds. Meanwhile, photophysical properties of the three complexes have also been discussed. Furthermore, the fluorescence behaviors of the two Cu(II) complexes in DMF are discussed.

© 2016 Elsevier Ltd. All rights reserved.

## 1. Introduction

The coordination chemistry of transition metal complexes with Salen-type ligands has achieved a considerable attention in the last decades [1–9], because of their redox-chemistry, unusual magnetic and structural properties, as well as their usage as models for metalloproteinase [10–18], and catalysts for oxidation and polymerization reactions [10,13,14,19]. It is important to introduce suitable functional groups into the organic moiety of the ligands in order to improve or tune the properties of these metal complexes [20–28]. Of particular is the steric and electronic effects of the substituents of salicylic and aniline rings which are the key factors in various reactions such as the epoxidation, symmetrical or asymmetrical Salen-based catalysis, polymerization catalysis and the electron transfer reactivity of the metal atoms with ligands bearing bulky tert-butyl substituents. For instance, symmetrical or asymmetrical Salen catalysts and electron-donating and -withdrawing groups are utilized to fine tune the nonlinear optical properties of the Cu(II) complexes of the Salen analogues. There are also some reports on the modification of the methylene chain length of the Salen complexes, including longer Salen analogues (trialkylene,

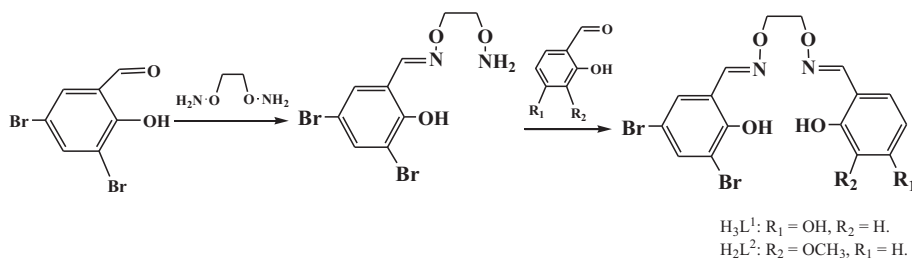
tetraalkylene, or longer alkylene chains) [29]. The chain length of the Salen complexes is one of the important factors that affect the electrochemical and spectroscopic properties of the central metal. Photoluminescence has been one of the highlights in modern coordination chemistry owing to potential applications in luminescent devices [30], which have been also observed for Salen-type compounds and their transition metal complexes [31–35]. In recent years, Cu(II) complexes with Salen-type ligands have drawn much attention for their photoluminescent characteristics [36,37].

Selective syntheses of these asymmetrical ligands is important because electronic and steric effects of the ligands on Salen-metal-assisted catalysis may be controlled by the introduction of different substituents into the two benzene rings [38]. It has been reported that metal complexes derived from asymmetrical Salamo-type ligands sometimes exhibit better enantioselectivities when compared with their symmetric counterparts [39].

In this paper, we describe the syntheses, spectroscopic characterization and fluorescent properties of the newly designed asymmetric Salamo-type ligands,  $\text{H}_3\text{L}^1$  and  $\text{H}_2\text{L}^2$  and their Cu(II) and Co(II) complexes.

\* Corresponding author.

E-mail address: [dongwk@126.com](mailto:dongwk@126.com) (W.-K. Dong).



**Scheme 1.** The synthetic route of two asymmetric Salamo-type ligands.

## 2. Experimental

### 2.1. Materials and instruments

3,5-Dibromo-2-hydroxybenzaldehyde, 2,4-dihydroxybenzaldehyde and 2-hydroxy-3-methoxybenzaldehyde were purchased from Aldrich and used without further purification. Other reagents and solvents were analytical grade reagents from Tianjin Chemical Reagent Factory.

C, H, and N analyses were obtained using a GmbH VarioEL V3.00 automatic elemental analysis instrument. Elemental analyses for metals were detected by an IRIS ER/SWP-1 ICP atomic emission spectrometer. FT-IR spectra were recorded on a VERTEX70 FT-IR spectrophotometer, with samples prepared as KBr ( $500\text{--}4000\text{ cm}^{-1}$ ) and CsI ( $100\text{--}500\text{ cm}^{-1}$ ) pellets. UV-Vis absorption and fluorescence spectra were recorded on a Shimadzu UV-2550 spectrometer and Perkin-Elmer LS-55 spectrometer, respectively.  $^1\text{H}$  NMR spectra were determined by German Bruker AVANCE DRX-400 spectrometer. Melting points were obtained by the use of an X4 microscopic melting point apparatus made in Beijing Taiké Instrument Limited Company and the thermometer was uncorrected. X-ray single-crystal structures were determined on a Bruker Smart APEX CCD area detector.

### 2.2. Syntheses of $H_3L^1$ and $H_2L^2$

The synthetic route to two asymmetric Salamo-type ligands  $H_3L^1$  and  $H_2L^2$  is shown in Scheme 1.

1,2-Bis(aminooxy)ethane was synthesized according to reported methods [36,40]. Yield, 78.4%. *Anal. Calc.* for  $C_2H_8N_2O_2$ : C, 26.08; H, 8.76; N, 30.42. Found: C, 25.96; H, 8.90; N, 30.35%.

Initially, the intermediate compound, monooxime 2-hydroxy-3,5-dibromobenzaldehyde *O*-(2-(aminooxy)ethyl) oxime was prepared by the reaction of 3,5-dibromo-2-hydroxybenzaldehyde (4 mmol) in ethanol (80 mL) with excess 1,2-bis(aminooxy)ethane (8 mmol) in ethanol (60 mL), and was heated at  $50\text{--}55\text{ }^\circ\text{C}$  for 6 h. The obtained mixture contained the desired monooxime and a small amount of dioxime. The pure monooxime was obtained after silica gel chromatographic ( $\text{SiO}_2$ , chloroform/ethyl acetate, 20:1) separation of the crude product, and was obtained as stable crystals. Yield, 61.6%. m.p.  $100\text{--}102\text{ }^\circ\text{C}$ . *Anal. Calc.* for  $C_9H_{10}Br_2N_2O_3$ : C, 30.54; H, 2.85; N, 7.91. Found: C, 30.59; H, 2.79; N, 7.87%.  $^1\text{H}$  NMR (400 MHz,  $\text{CDCl}_3$ ): 3.98 (t,  $J = 4.5$  Hz, 2H), 4.39 (t,  $J = 4.5$  Hz, 2H), 5.54 (brs, 2H), 6.89 (d,  $J = 9.0$  Hz, 1H), 7.36 (dd,  $J = 9.0, 2.5$  Hz, 1H), 8.12 (s, 1H), 9.85 (s, 1H).

Finally, the asymmetrical Salamo derivative product, 5-hydroxy-4',6'-dibromo-2,2'-[ethylenediyl]dioxibis(nitrilomethyl)

**Table 1**  
Crystal data and structure refinement for complexes **1**, **2** and **3**.

|  |  |   |  |
|--|--|---|--|
| CCDC deposit number  | 1433366  | 1433367   | 1433368  |
| Empirical formula  | $C_{16}H_{12}Br_2CuN_2O_5$                                   | $C_{17}H_{16}Br_2CuN_2O_6$                                  | $C_{40}H_{37}Br_4Co_2N_7O_{10}$                              |
| Formula weight   | 535.64   | 567.67  | 1213.27  |
| $T$ (K)  | 293(2)   | 298(2)  | 293(2)   |
| $\lambda$ (Å)  | 0.71073  | 0.71073   | 0.71073  |
| Crystal system   | monoclinic   | monoclinic  | triclinic  |
| Space group  | $P 2(1)/c$   | $P 2(1)/c$  | $P\bar{1}$   |
| <i>Unit cell dimensions</i>                                |  |   |  |
| $a$ (Å)  | 16.3506(15)  | 11.1458(9)  | 11.8954(14)  |
| $b$ (Å)  | 10.2289(7)   | 13.6328(12)   | 14.3538(14)  |
| $c$ (Å)  | 10.7001(11)  | 13.0070(13)   | 14.3855(16)  |
| $\alpha$ ( $^\circ$ )                                      | 92.8420(10)  | 90  | 94.5440(10)  |
| $\beta$ ( $^\circ$ )                                       | 90.00  | 98.9240(10)   | 104.731(2)   |
| $\gamma$ ( $^\circ$ )                                      | 104.839(2)   | 90  | 98.8210(10)  |
| $V$ (Å <sup>3</sup> )                                      | 1729.9(3)  | 1952.5(3)   | 2329.4(4)  |
| $Z$  | 4  | 2   | 2  |
| $D_{\text{calc}}$ (Mg/m <sup>3</sup> )                     | 2.057  | 1.931   | 1.730  |
| $\mu$ (mm <sup>-1</sup> )                                  | 5.913  | 5.249   | 4.204  |
| $F(000)$   | 1044   | 1116  | 1200   |
| Crystal size (mm)  | $0.20 \times 0.11 \times 0.06$                               | $0.34 \times 0.32 \times 0.30$                              | $0.43 \times 0.23 \times 0.14$                               |
| $\theta$ ( $^\circ$ )                                      | 2.58–25.01   | 2.69–25.02  | 2.55–25.02   |
| Index ranges   | $-19 \leq h \leq 19, -12 \leq k \leq 11, -12 \leq l \leq 12$ | $-9 \leq h \leq 13, -16 \leq k \leq 14, -15 \leq l \leq 15$ | $-14 \leq h \leq 14, -12 \leq k \leq 17, -17 \leq l \leq 16$ |
| Reflections collected                                      | 9339   | 9613  | 14615  |
| Independent reflections ( $R_{\text{int}}$ )               | 3058 (0.0638)  | 3438 (0.0602)   | 8203 (0.0861)  |
| Completeness to $\theta = 25.02$ (%)                       | 99.9   | 99.6  | 99.9   |
| Data/restraints/parameters                                 | 3058/0/235   | 3438/0/254  | 8203/0/573   |
| Goodness of fit (GOF) on $F^2$                             | 1.071  | 1.034   | 1.014  |
| $R_1$  | 0.0453   | 0.0451  | 0.0702   |
| $wR_2$ [ $I > 2\sigma(I)$ ]                                | 0.0977   | 0.1002  | 0.1236   |
| $\Delta\rho_{\text{maximum,minimum}}$ (e Å <sup>-3</sup> ) | 0.772 and $-0.777$   | 0.843 and $-0.572$  | 0.862 and $-0.621$   |

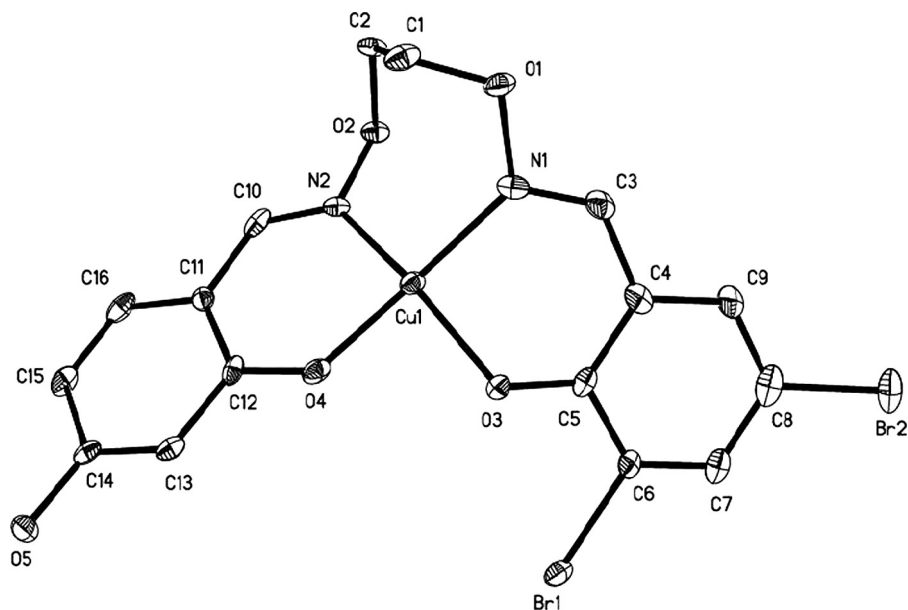


Fig. 1. Molecular structure of complex **1** with the atom numbering. Thermal ellipsoids are plotted at 30% probability level.

Table 2

Selected bond distances (Å) and bond angles (°) for complexes **1**, **2** and **3**.

| Bond   | Distance  | Bond      | Distance  | Bond      | Distance   |
|--|-----------|-----------|-----------|-----------|------------|
| <b>1</b>   |           |           |           |           |            |
| Cu1–O3   | 1.921(4)  | Cu1–O4    | 1.883(5)  | Cu1–N1    | 1.996(6)   |
| Cu1–N2   | 1.920(5)  |           |           |           |            |
| <b>2</b>   |           |           |           |           |            |
| Cu1–O3   | 1.939(4)  | Cu1–N1    | 1.963(6)  | Cu1–O6    | 2.240(4)   |
| Cu1–O5   | 1.941(5)  | Cu1–N2    | 2.028(5)  |           |            |
| <b>3</b>   |           |           |           |           |            |
| Co1–O3   | 1.923(8)  | Co1–O9    | 1.972(6)  | Co1–N1    | 2.056(8)   |
| Co1–O4   | 2.075(6)  | Co1–N2    | 2.081(8)  | Co2–O8    | 1.908(7)   |
| Co2–O4   | 1.992(6)  | Co2–N3    | 2.048(8)  | Co2–N4    | 2.074(9)   |
| Co2–O9   | 2.086(6)  |           |           |           |            |
| Bond   | Angle     | Bond      | Angle     | Bond      | Angle      |
| <i>[Cu(HL<sup>1</sup>)]</i>  |           |           |           |           |            |
| O4–Cu1–N2  | 92.4(2)   | O4–Cu1–N1 | 157.6(2)  | N2–Cu1–N1 | 99.1(2)    |
| O4–Cu1–O3  | 88.54(19) | N2–Cu1–O3 | 152.6(2)  | O3–Cu1–N1 | 89.9(2)    |
| <i>[Cu(L<sup>2</sup>)H<sub>2</sub>O]</i>                             |           |           |           |           |            |
| O3–Cu1–O5  | 87.52(18) | O5–Cu1–N2 | 89.2(2)   | O5–Cu1–O6 | 103.29(18) |
| O3–Cu1–N1  | 87.7(2)   | N1–Cu1–N2 | 95.0(2)   | N1–Cu1–O6 | 96.5(2)    |
| O5–Cu1–N1  | 159.7(2)  | O3–Cu1–O6 | 91.10(17) | N2–Cu1–O6 | 90.67(19)  |
| O3–Cu1–N2  | 176.6(2)  |           |           |           |            |
| <i>[Co<sub>2</sub>(L<sup>2</sup>)<sub>2</sub>·3CH<sub>3</sub>CN]</i> |           |           |           |           |            |
| O3–Co1–O9  | 120.7(3)  | O9–Co1–O4 | 76.3(2)   | N1–Co1–N2 | 91.5(3)    |
| O3–Co1–N1  | 89.7(4)   | N1–Co1–O4 | 169.4(4)  | O4–Co1–N2 | 81.1(3)    |
| O9–Co1–N1  | 102.4(3)  | O3–Co1–N2 | 110.5(3)  | O8–Co2–O4 | 122.8(3)   |
| O3–Co1–O4  | 100.1(3)  | O9–Co1–N2 | 126.7(3)  | O8–Co2–N3 | 89.8(3)    |
| O4–Co2–N3  | 102.4(3)  | O8–Co2–N4 | 109.3(3)  | O4–Co2–N2 | 125.9(3)   |
| N3–Co2–N4  | 90.8(4)   | O8–Co2–O9 | 101.1(3)  | O4–Co2–O9 | 75.6(3)    |
| N3–Co2–O9  | 168.1(4)  | N4–Co2–O9 | 81.4(3)   |           |            |

dyne)diphenol (H<sub>3</sub>L<sup>1</sup>) was obtained by the reaction of 2-hydroxy-3,5-dibromobenzaldehyde *O*-(2-(aminooxy)ethyl) oxime (1 mmol) in ethanol (20 mL) with appropriate 2,4-dihydroxybenzaldehyde (1 mmol) in ethanol (20 mL), and was heated at 50–55 °C for 5 h and yielded pale pink H<sub>3</sub>L<sup>1</sup> powder. Yield, 68.3%. m.p. 127–128 °C. *Anal. Calc.* for C<sub>16</sub>H<sub>14</sub>Br<sub>2</sub>N<sub>2</sub>O<sub>5</sub>: C, 40.53; H, 2.98; N, 5.91. Found: C, 40.60; H, 2.89; N, 5.96%. <sup>1</sup>H NMR (400 MHz, DMSO-d<sub>6</sub>): 4.48–4.50 (m, 4H, CH<sub>2</sub>), 6.88 (d, *J* = 8.6 Hz, 1H), 6.92 (t, *J* = 7.8 Hz, 1H), 6.98 (d, *J* = 7.8 Hz, 1H), 7.16 (dd, *J* = 7.8 Hz, 1.5 Hz,

1H), 7.35 (dd, *J* = 8.6 Hz, 2.5 Hz, 1H), 8.16 (s, 1H), 8.23 (s, 1H), 9.72 (s, 1H), 9.77 (s, 1H), 10.38 (s, 1H).

The second asymmetrical Salamo-type ligand, 6-methoxy-4',6'-dibromo-2,2'-(ethylenedioxybis(nitrilomethylidyne))diphenol (H<sub>2</sub>L<sup>2</sup>) was synthesized according to the analogous method described above [37,41]. Yield, 75.2%. m.p. 137–138 °C. *Anal. Calc.* for C<sub>17</sub>H<sub>16</sub>Br<sub>2</sub>N<sub>2</sub>O<sub>5</sub>: C, 41.83; H, 3.30; N, 5.74. Found: C, 41.91; H, 3.41; N, 5.66%. <sup>1</sup>H NMR (400 MHz, DMSO-d<sub>6</sub>, δ, ppm): 3.92 (s, 3H), 4.46–4.49 (m, 4H, CH<sub>2</sub>), 6.88 (d, *J* = 8.6 Hz, 1H), 6.92 (t,

$J = 7.8$  Hz, 1H), 6.96 (d,  $J = 7.8$  Hz, 1H), 7.14 (dd,  $J = 7.8$  Hz, 1.5 Hz, 1H), 7.35 (dd,  $J = 8.6$  Hz, 2.5 Hz, 1H), 8.16 (s, 1H), 8.22 (s, 1H), 9.75 (s, 1H), 10.36 (s, 1H).

### 2.3. Synthesis of complex 1

A solution of Cu(II) acetate hydrate (1.9 mg, 0.01 mmol) in ethanol (2 mL) was added dropwisely to a solution of  $H_3L^1$  (4.75 mg, 0.01 mmol) in acetone (2 mL) at room temperature. Immediately the color turned dark-green, while the mixture was filtered and the filtrate allowed to stand at room temperature for about one month. The solvent was partially evaporated and red-brown prismatic crystals suitable for X-ray crystallographic analysis were obtained. Yield, 46.9%. *Anal. Calc.* for  $C_{16}H_{12}Br_2CuN_2O_5$  ( $[Cu(HL^1)]$ ): C, 35.88; H, 2.26; N, 5.23; Cu, 11.86. Found: C, 35.54; H, 2.36; N, 5.10; Cu, 11.90%.

### 2.4. Synthesis of complex 2

A solution of Cu(II) acetate hydrate (1.9 mg, 0.01 mmol) in methanol/acetonitrile (2:1) (3 mL) was added dropwisely to a solution of  $H_2L^2$  (4.88 mg, 0.01 mmol) in acetone (2 mL) at room temperature. The color of the mixed solution immediately turned brown, the mixture was filtered and the filtrate allowed to stand at room temperature for about three weeks. The solvent was partially evaporated and several dark-brown block-like single crystals suitable for X-ray crystallographic analysis were obtained. Yield, 53.9%. *Anal. Calc.* for  $C_{17}H_{16}Br_2CuN_2O_6$  ( $[Cu(L^2)H_2O]$ ): C, 35.97; H, 2.84; N, 4.93; Cu, 11.19. Found: C, 35.85; H, 2.76; N, 5.23; Cu, 11.26%.

### 2.5. Synthesis of complex 3

A solution of cobalt(II) acetate tetrahydrate (2.48 mg, 0.010 mmol) in methanol (3 mL) was added dropwisely to a solution of  $H_2L^2$  (4.88 mg, 0.1 mmol) in acetonitrile (3 mL) at room temperature. The color of the solution immediately turned pale yellow, and the mixture was allowed to stand at room temperature for about two weeks. After the solvent was partially evaporated, several brown block-shaped single crystals suitable for X-ray crystallographic analysis were obtained. The crystal was unstable, easily weathered in the air. Yield, 66.3%. *Anal. Calc.* for  $C_{40}H_{37}Br_4-$

$Co_2N_7O_{10}$  ( $[Co_2(L^2)_2] \cdot 3CH_3CN$ ): C, 39.60; H, 3.07; N, 8.08; Co, 9.71. Found: C, 38.98; H, 3.01; N, 8.24; Co, 9.56%.

### 2.6. X-ray crystal structure determination

The single crystals of the complexes  $[Cu(HL^1)]$  (**1**),  $[Cu(L^2)H_2O]$  (**2**) and  $[Co_2(L^2)_2] \cdot 3CH_3CN$  (**3**) with approximate dimensions of  $0.20 \times 0.11 \times 0.06$  mm<sup>3</sup>,  $0.34 \times 0.32 \times 0.30$  mm<sup>3</sup> and  $0.43 \times 0.23 \times 0.14$  mm<sup>3</sup>, respectively, were placed on a Bruker Smart 1000 CCD area detector. The diffraction data were collected using a graphite monochromated Mo  $K\alpha$  radiation ( $\lambda = 0.71073$  Å) at 298(2) K, 298(2) K and 293(2) K for **1**, **2** and **3**, respectively. The structures were solved by using the program SHELXL-97 and Fourier difference techniques, and refined by full-matrix least-squares method on  $F^2$ . All hydrogen atoms were added theoretically. The crystal and experimental data are shown in Table 1.

## 3. Results and discussion

### 3.1. Crystal structures

#### 3.1.1. The crystal structure and supramolecular interactions of $[Cu(HL^1)]$ , **1**

The crystal structure of the Cu(II) complex, **1** is shown in Fig. 1. The Selected bond distances (Å) and bond angles (°) for the three complexes are listed in Table 2.

The complex **1** crystallizes in the monoclinic, space group  $P2(1)/c$  with  $Z = 4$ . The molecular structure of **1** consists of one Cu(II) atom and one deprotonated  $(HL^1)^{2-}$  unit. In fact, this mononuclear Cu(II) complex is similar to the previously reported Salen or Salamo-type complexes [41], for instance, the Cu(II) atoms of  $[Cu(Salamo)]$ ,  $[Cu(3-MeOSalamo)]$  ( $H_2Salamo = 1,2$ -bis(salicylideneaminoxy)ethane) [42] and  $[Cu(PnSalen)]$  [43] have a square planar geometry. The coordination geometry around Cu(II) atom can be best described as a slight distortion toward tetrahedral geometry from the square planar structure, where the Cu(II) atom lies in *cis*- $N_2O_2$  cavity by two oxime nitrogen (N1 and N2) atoms and two phenoxo oxygen (O3 and O4) atoms.

In the complex **1**, the dihedral angle between the coordination planes of  $N1-Cu1-O3$  and  $N2-Cu1-O4$  is  $34.36(4)^\circ$ , which is larger than that of the reported complexes with symmetric Salen-type bisoxime ligands [44]. This significant enlargement indicates that the  $(HL^1)^{2-}$  unit has serious distortion probably as a result of its

**Table 3**  
Hydrogen bonding distances (Å) and bond angles (°) for complexes **1**, **2** and **3**.

| D–H...A        | d(D–H) | d(H–A) | d(D–A)    | $\angle D-H-A$ | Type  | Symmetry code        |
|----------------|--------|--------|-----------|----------------|-------|----------------------|
| <b>1</b>       |        |        |           |                |       |                      |
| O5–H5...O3     | 0.82   | 1.98   | 2.715(6)  | 149            | Inter | $1-x, 1-y, 1-z$      |
| C1–H1A...O3    | 0.97   | 2.51   | 3.380(8)  | 149            | Inter | $x, 1/2-y, 1/2+z$    |
| C13–H13...O4   | 0.93   | 2.6    | 3.521(8)  | 169            | Inter | $1-x, 1-y, 1-z$      |
| C16–H16...O5   | 0.93   | 2.59   | 3.490(8)  | 162            | Inter | $1-x, -1/2+y, 1/2-z$ |
| <b>2</b>       |        |        |           |                |       |                      |
| O6–H6C...O3    | 0.85   | 2.1    | 2.837(6)  | 144            | Inter | $1-x, 1-y, 1-z$      |
| O6–H6C...O4    | 0.85   | 2.2    | 2.867(7)  | 135            | Inter | $1-x, 1-y, 1-z$      |
| O6–H6D...O5    | 0.85   | 2.14   | 2.871(6)  | 144            | Inter | $1-x, 1-y, 1-z$      |
| O6–H6D...Br1   | 0.85   | 2.82   | 3.380(4)  | 125            | Inter | $1-x, 1-y, 1-z$      |
| C11–H11...O3   | 0.93   | 2.38   | 3.305(8)  | 172            | Inter | $x, 3/2-y, 1/2+z$    |
| C17–H17...O4   | 0.93   | 2.61   | 3.390(9)  | 141            | Inter | $x, 3/2-y, -1/2+z$   |
| <b>3</b>       |        |        |           |                |       |                      |
| C17–H17A...O6  | 0.96   | 2.59   | 3.521(14) | 163            | Inter | $1-x, 1-y, 1-z$      |
| C34–H34A...O1  | 0.96   | 2.65   | 3.527(1)  | 152            | Inter | $1-x, 2-y, -z$       |
| C9–H9...O1     | 0.93   | 2.72   | 3.249(1)  | 117            | Inter | $1-x, 2-y, -z$       |
| C19–H19A...N5  | 0.97   | 2.63   | 3.220(6)  | 120            | Inter | $1+x, y, z$          |
| C36–H36A...Br3 | 0.96   | 2.93   | 3.816(11) | 154            | Intra |                      |
| C36–H36B...O4  | 0.96   | 2.7    | 3.632(1)  | 163            | Intra |                      |

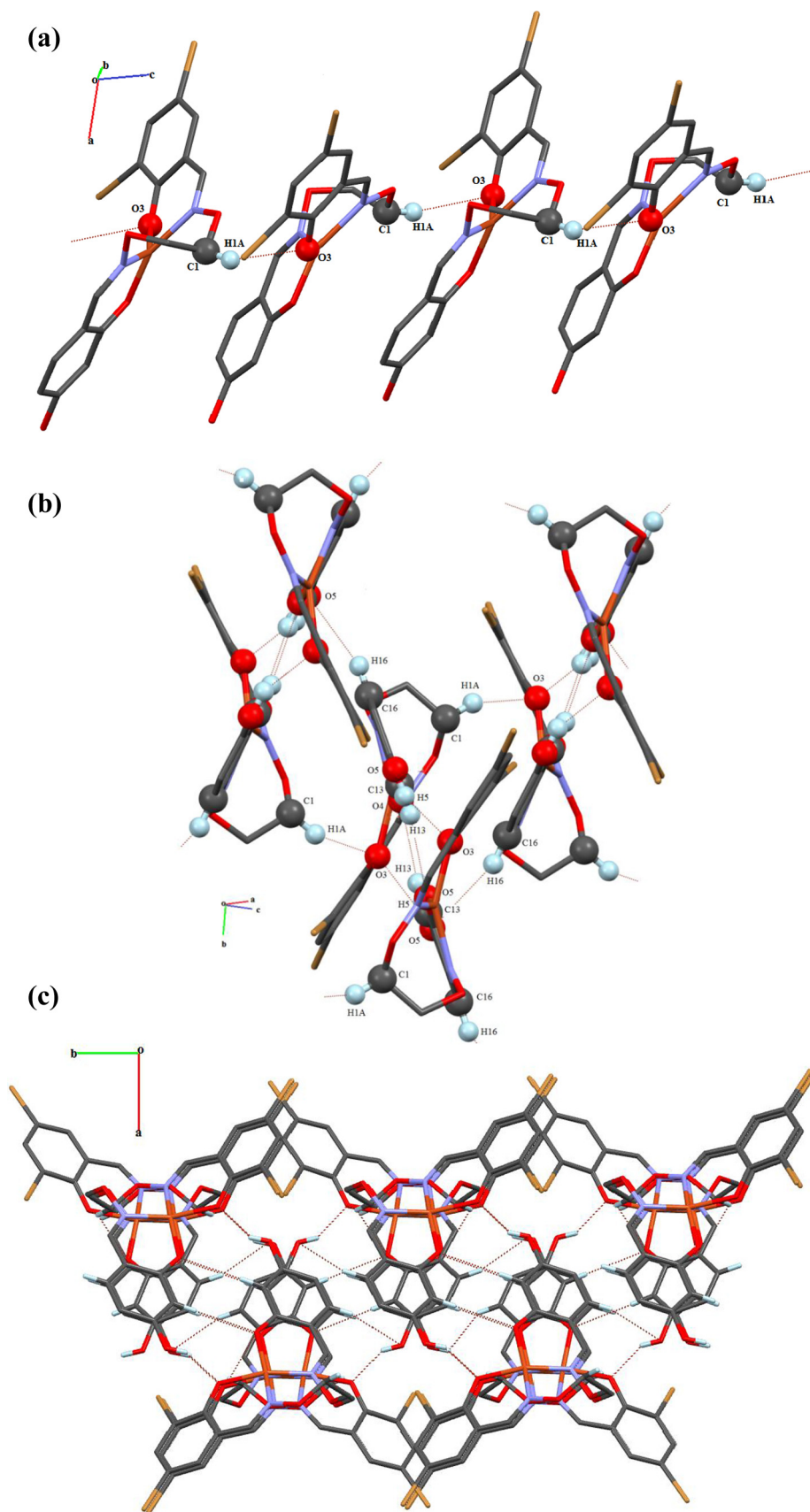


**Fig. 2.** Supramolecular structures of  $[\text{Cu}(\text{HL}^1)]$ . (a) View of the 1D chain motif within complex 1 along the  $c$  axis; (b) View of the 2D layered motif along the  $bc$  plane; (c) Part of 3D supramolecular network through intermolecular interactions.

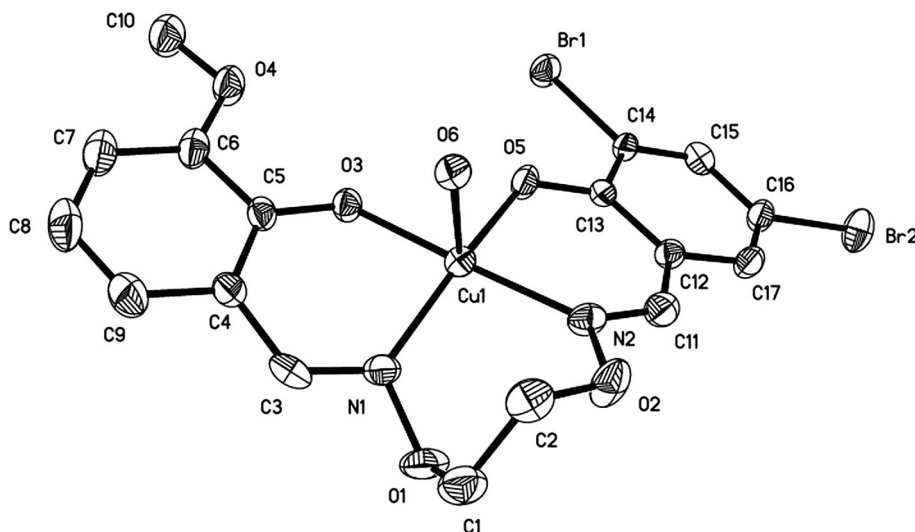


Fig. 3. Molecular structure of complex **2** with the atom numbering. Thermal ellipsoids are plotted at 30% probability level.

asymmetry. Meanwhile, the dihedral angle between the mean plane of Cu–O3–C5–C4–C3–N1 and its adjacent phenyl ring is  $9.30(3)^\circ$  while Cu–O4–C12–C11–C10–N2 and its adjacent phenyl ring is  $3.61(3)^\circ$ . Furthermore, the deviation of Cu1 atom from the  $N_2O_2$  coordination plane is  $0.046(2)$  Å while those of the four donor (N1, N2, O3 and O4) atoms from their mean plane are  $0.373(3)$ ,  $-0.376(4)$ ,  $-0.428(3)$  and  $0.432(3)$  Å, respectively. All show that the Salamo-type  $(HL^1)^{2-}$  moiety is not planar, but has a twisted geometry.

Notably, there are a large number of intermolecular hydrogen bonds in the complex **1**. The hydrogen bond data are summarized in Table 3. Complex **1** shows the existence of a weak intramolecular C1–H1A...O3 hydrogen bond between the methylene groups from the O-alkyl chain of  $(HL^1)^{2-}$  unit and phenolic oxygen (O3) atom. The complex monomer links adjacent molecules through C1–H1A...O3 hydrogen bond interactions into an infinite 1D supramolecular chain along the *a*-axis (Fig. 2a). Furthermore, this linkage is further stabilized by three pairs of intermolecular O(5)–H(5)...O(3), C(13)–H(13)...O(4) and C(16)–H(16)...O(5) interactions to form an infinite 2D-layer supramolecular structure (Fig. 2b). Thus, every complex **1** molecule links the other adjacent molecules into a novel 3D supramolecular network structure through these intermolecular interactions (Fig. 2c).

### 3.1.2. The crystal structure and supramolecular interactions of $[Cu(L^2)H_2O]$ , **2**

The crystal structure of complex **2** is shown in Fig. 3. The complex consists of one Cu(II) atom, one  $(L^2)^{2-}$  unit and one coordinated water molecule, and crystallizes in the monoclinic, space group  $P2(1)/c$  with  $Z = 2$ . X-ray crystallographic analysis of complex **2** reveals a mononuclear structure which is different from the earlier reported structures of 1:2 [36], 2:2 [45–47], 2:3 [48] and 2:4 [48] (L: Cu(II)) in the Salamo-type Cu(II) complexes. The complex **2**,  $[Cu(L^2)H_2O]$  with the Salamo-type ligand  $H_2L^2$  was obtained from methanol/acetonitrile/acetone solution as an aqua complex, whereas some of the other Salamo [41] and related (Salen [49], Saltn [50,51], Salbn [52] etc) complexes had a tetracoordinate structure without aqua ligands. The value of  $\tau = 0.28$  clearly indicates that the coordination environment of the Cu(II) atom can be best described as a square-pyramidal topology with the Cu(II) atom being penta-coordinated. The two phenolic oxygen atoms (O3 and O5) and the two oxime nitrogen atoms (N1 and N2) of the  $(L^2)^{2-}$  unit constitute the basal plane (Cu1–O3,  $1.939(4)$  Å;

Cu1–O5,  $1.941(5)$  Å; Cu1–N1,  $1.963(6)$  Å; Cu1–N2,  $2.028(5)$  Å), and one oxygen atom (O6) of the coordinated water molecule occupies the axial position (Cu1–O8,  $2.240(4)$  Å). The axial bond distance Cu1–O6 is longer than all of the others which formed the basal plane. More typical Cu–O bond length of the apical water molecule in such square pyramidal molecule is the value of  $2.369(2)$  Å found in  $[Cu(MeO-Salen)(H_2O)]$  [53].

Four coordination atoms in the basal plane are deviated slightly from the mean plane, with N2 and O3 above average by  $0.144(3)$  Å and  $0.163(3)$  Å, and N1 and O5 below average by  $0.148(3)$  Å and  $0.158(3)$  Å, respectively. Meanwhile, the Cu(II) atom is  $0.181(3)$  Å displaced from the mean plane. The dihedral angle between the coordination plane of O3–Cu1–N1 and that of O5–Cu1–N2 is  $19.77(3)^\circ$ . In addition, the mean plane ( $N_2O_2$ ) and sal(1) (2-hydroxy-3-methoxybenzaldehyde) have a dihedral angle of  $18.25(3)^\circ$ , and the dihedral angle of sal(2) (3,5-dibromo-2-hydroxybenzaldehyde) with the mean plane is  $29.65(4)^\circ$ . These could be attributed to the asymmetric composition too.

The introduction of a coordinated water molecule in complex **2** successfully leads to the assembly of dimer units by intermolecular hydrogen bonds. As illustrated in Fig. 4a, four intermolecular hydrogen bonds, O6–H6C...O3, O6–H6C...O4, O6–H6D...O5 and O6–H6D...Br1 are formed. One of the water protons –O6H6C of the coordinated water molecule in complex **2** is hydrogen-bonded to phenolic oxygen atom (O3) and methoxy oxygen atom (O4) of  $(L^2)^{2-}$  unit of the adjacent molecule. The other of water proton –O6H6D of the coordinated water molecule is bound to the coordinated phenolic oxygen atom (O5) and the bromo atom (Br1) of the  $(L^2)^{2-}$  unit of the adjacent molecule. Consequently, these hydrogen bonding interactions have stabilized a pair of the Cu(II) complex molecules to form a dimer with the nearest Cu...Cu distance of  $4.839(4)$  Å [54]. Moreover, there exists two weak intermolecular C11–H11...O3 and C17–H17...O4 hydrogen bond interactions. Simultaneously, each complex **2** molecule is connected to adjacent molecules forming a Zigzag chain along the *c*-axis (Fig. 4b). Thus, each dimer molecule links four other molecules into an infinite 2D supramolecular network via intermolecular O–H...O, C–H...O and O–H...Br hydrogen bond interactions (Fig. 4c).

### 3.1.3. The crystal structure and supramolecular interactions of $[Co_2(L^2)_2] \cdot 3CH_3CN$ , **3**

X-ray crystallographic analysis reveals that the Co(II) dimer consists of two Co(II) atoms, two deprotonated  $(L^2)^{2-}$  units and

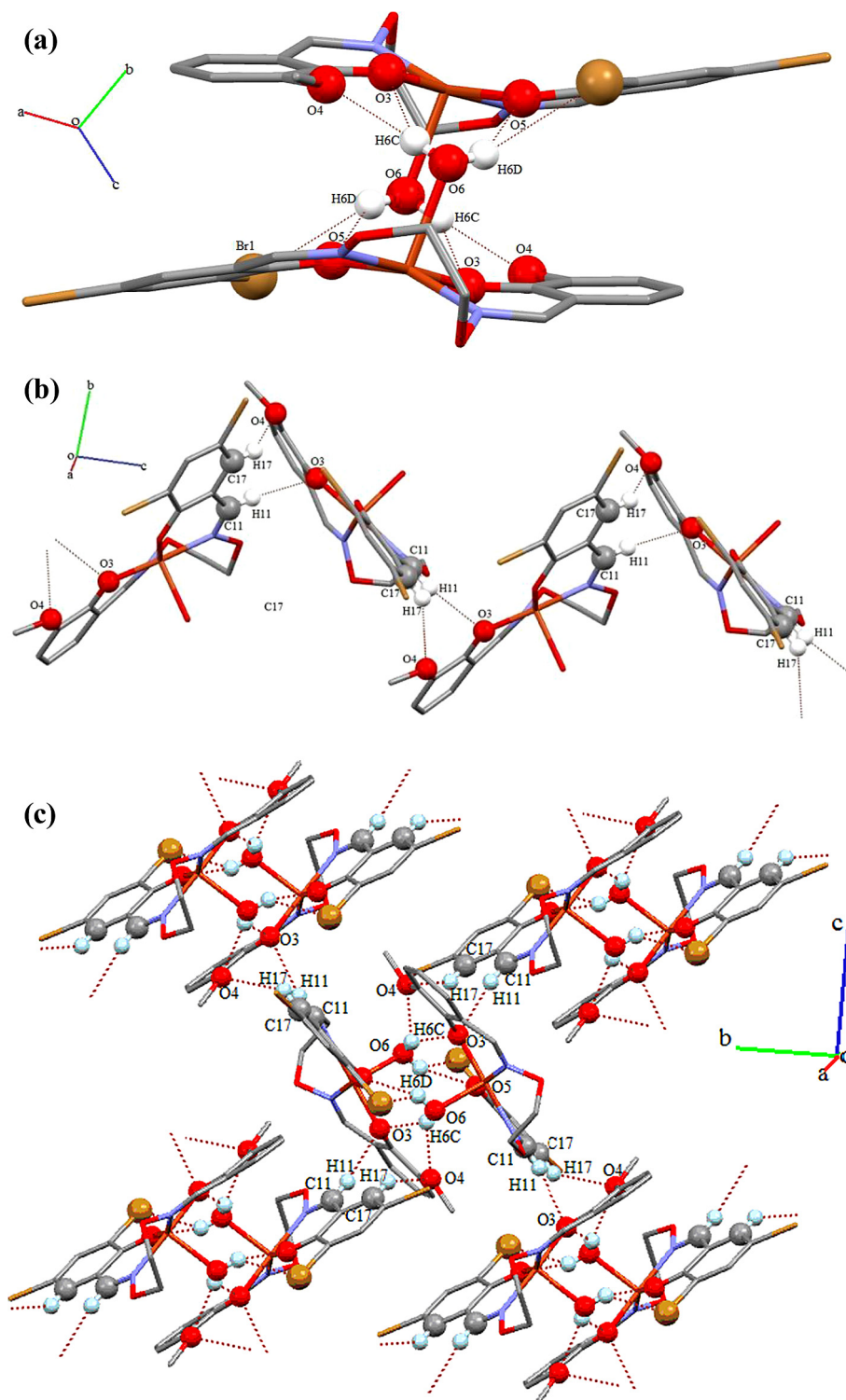


**Fig. 4.** Supermolecular structures of complex **2**. (a) A dimeric unit formed by intermolecular hydrogen bonds. (b) View of the 1D chain motif within the complex along the *a* axis; (c) View of the 2D-layered motif along the *bc* plane.

three uncoordinated acetonitrile molecules (Fig. 5). The complex **3** crystallizes in the triclinic, space group  $P\bar{1}$  with  $Z = 2$ . The structure of complex **3** can be described as two  $[\text{Co}(\text{L}^2)]$  unit connected by a diphenoxy-bridge. Two Co(II) atoms sit in the Salamo moiety, two oxygen atoms (O4 and O9) bridge two Co(II) atoms. To the best of our knowledge, the novel 2:2  $(\text{L}^2)^{2-}:\text{Co}(\text{II})$  Salamo-type Co(II) complex is rarely found reported in comparison to the Salamo-type Co(II) complexes having the structures of 1:1 [55,56], 2:3

[55,57,58] and 4:8 [38] (L: Co(II)). The Co1 atom has a trigonal-bipyramidal geometry ( $\tau = 0.712$ ), whose axial positions are occupied by the N1 and O4 donor atoms. Three coordinated atoms (O9–N2–O3) form the basal plane and the Co1 deviates from the mean plane by 0.170(3) Å. The dihedral angle of O(3)–Co(1)–N(1) and O(4)–Co(1)–N(2) is 69.92(4)°, which indicates that  $(\text{L}^2)^{2-}$  unit has serious distortion probably due to its asymmetry. The geometry of Co2 is similar to that of Co1. The value of  $\tau = 0.703$  clearly shows

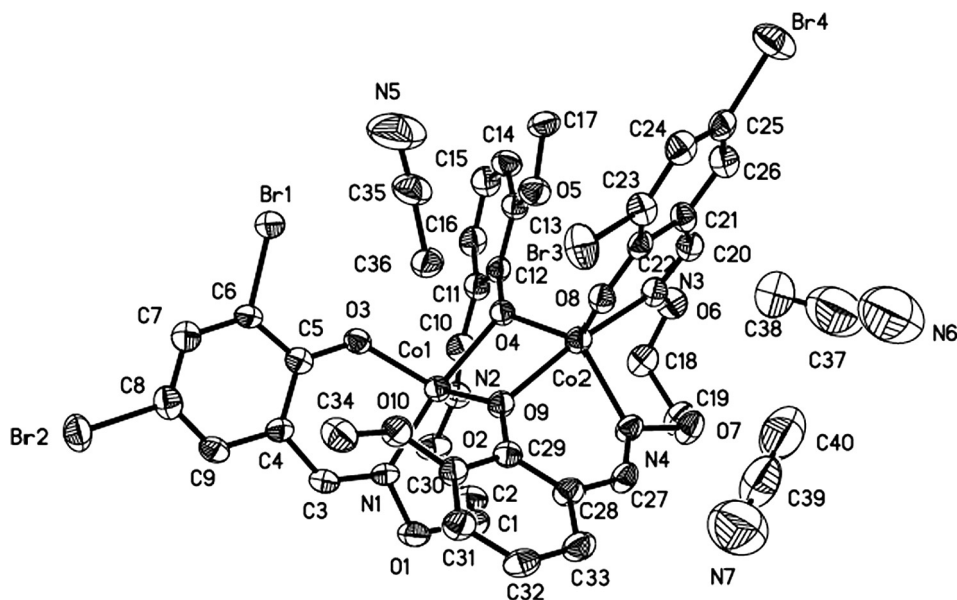


Fig. 5. Molecular structure of complex **3** with the atom numbering. Thermal ellipsoids are plotted at 30% probability level.

that the coordination environment of the Co2 atom is close to trigonal bipyramidal geometry in which the axial site is occupied by O9 and N3 atoms. The dihedral angle between the coordination plane of O(8)–Co(2)–N(3) and that of O(4)–Co(2)–N(4) is 71.17 (4)°. This is different from the reported structures of its analogues Cu(Salen) [59] and Cu(Salamo) [41], which form slightly pyramidalized square planar geometries, and could be stabilized by the intermolecular contacts between copper and oxygen atoms to form a head-to-tail dimer.

The special thing about Co(II) dimer lies in its self-assembly array linked by intramolecular and intermolecular hydrogen bonds. As a result of the three uncoordinated acetonitrile, complex **3** supramolecular structure experiences a huge change. The Co(II) dimer via three intermolecular C(17)–H(17A)···O(6), C(34)–H(34A)···O(1) and C(9)–H(9)···O(1) hydrogen bonds links neighboring molecules into an infinite 1D chain supramolecular structure along the *c* axis (Fig. 6a). Interestingly, an unconnected acetonitrile molecule provides a hydrogen bond donor and acceptor. Thus, this linkage is further stabilized by one intermolecular hydrogen bond C(19)–H(19A)···N(5) and two pairs of intramolecular hydrogen bonds C(36)–H(36A)···Br(3), C(36)–H(36B)···O(4) to form an infinite 2D supramolecular layered structure (Fig. 6b).

### 3.2. FT-IR spectra analysis

The IR spectra of the free ligands H<sub>3</sub>L<sup>1</sup> and H<sub>2</sub>L<sup>2</sup> and their corresponding Cu(II) and Co(II) complexes exhibit various bands in the 500–4000 cm<sup>-1</sup> region. The most important FT-IR bands for the ligands and the Cu(II) and Co(II) complexes are given in Table 4. The free ligands H<sub>3</sub>L<sup>1</sup> and H<sub>2</sub>L<sup>2</sup> exhibit characteristic C=N stretching bands at 1614 and 1622 cm<sup>-1</sup>, while those of complexes **1**, **2** and **3** are observed at 1605, 1601 and 1607 cm<sup>-1</sup>, respectively. The C=N stretching frequencies are shifted to lower frequencies by ca. 9, 11 and 15 cm<sup>-1</sup> for **1**, **2** and **3**, respectively, upon complexation, indicating a decrease in the C=N bond order due to the coordinated bonds of the Cu(II) and Co(II) atoms with the oxime nitrogen lone pair [57].

The Ar–O stretching frequency appears as a strong band within 1263–1213 cm<sup>-1</sup> range as reported for similar salen-type ligands. These bands occur at 1265 and 1246 cm<sup>-1</sup> for H<sub>3</sub>L<sup>1</sup> and H<sub>2</sub>L<sup>2</sup>, respectively. However, the Ar–O stretching frequencies are

observed at 1203, 1230 and 1244 cm<sup>-1</sup> for complexes **1**, **2** and **3**, respectively. The Ar–O stretching frequencies are shifted to lower frequencies, indicating that the M–O bonds are formed between the Cu(II) or Co(II) atoms and oxygen atoms of the phenolic groups. In addition, infrared spectrum of complex **2** shows the expected absorption bands at ca. 3415, 1636, and 547 cm<sup>-1</sup> which could be assigned to the coordinated water molecule, as is substantiated by the crystal structure, indicating the presence of one coordinated water molecule [57].

The far-infrared spectra of complexes **1**, **2** and **3** were also obtained in the region 500–100 cm<sup>-1</sup> in order to identify frequencies due to the M–O and M–N bonds. The IR spectra of the Cu(II) complexes show  $\nu_{(\text{Cu}-\text{N})}$  and  $\nu_{(\text{Cu}-\text{O})}$  vibration absorption frequencies at 511 cm<sup>-1</sup> and 439 cm<sup>-1</sup> for complex **1**, 495 cm<sup>-1</sup> and 423 cm<sup>-1</sup> for complex **2**, respectively [60], and complex **3** shows  $\nu_{(\text{Co}-\text{N})}$  and  $\nu_{(\text{Co}-\text{O})}$  vibration absorption frequencies at 489 cm<sup>-1</sup> and 446 cm<sup>-1</sup>, respectively. As pointed out by Percy and Thornton [61], the metal–oxygen and metal–nitrogen frequency assignments are at times very difficult.

### 3.3. UV–Vis absorption spectra study

The UV–Vis absorption spectra of the free ligands H<sub>3</sub>L<sup>1</sup> and H<sub>2</sub>L<sup>2</sup> and their corresponding complexes **1**, **2** and **3** were determined in 5.0 × 10<sup>-5</sup> mol L<sup>-1</sup> DMF solution, and are shown in Fig. 7a and b, respectively.

It can be seen that the absorption peaks of the three complexes **1**, **2** and **3** are obviously different from those of the free ligands H<sub>3</sub>L<sup>1</sup> and H<sub>2</sub>L<sup>2</sup> upon complexation. The UV–Vis absorption spectra of the free ligands consist of two relatively intense bands centered at 274 and 313 nm for H<sub>3</sub>L<sup>1</sup>, and 273 and 320 nm for H<sub>2</sub>L<sup>2</sup> which could be assigned to the  $\pi$ – $\pi^*$  transitions of the benzene rings of salicylaldehyde units [62]. Compared with the free ligands H<sub>3</sub>L<sup>1</sup> and H<sub>2</sub>L<sup>2</sup>, the absorption bands at 313 and 320 nm disappear from the UV–Vis spectra of complexes **1**, **2** and **3**, which indicate that the oxime nitrogen atoms are involved in coordination to the Cu(II) and Co(II) atoms [49]. The intraligand  $\pi$ – $\pi^*$  transitions of the benzene rings of salicylaldehyde units are slightly shifted in the corresponding complexes and appear at 293, 280 and 269 nm for complexes **1**, **2** and **3**, respectively. Moreover, the new absorption bands are observed at 364, 380 and 375 nm for complexes **1**, **2**

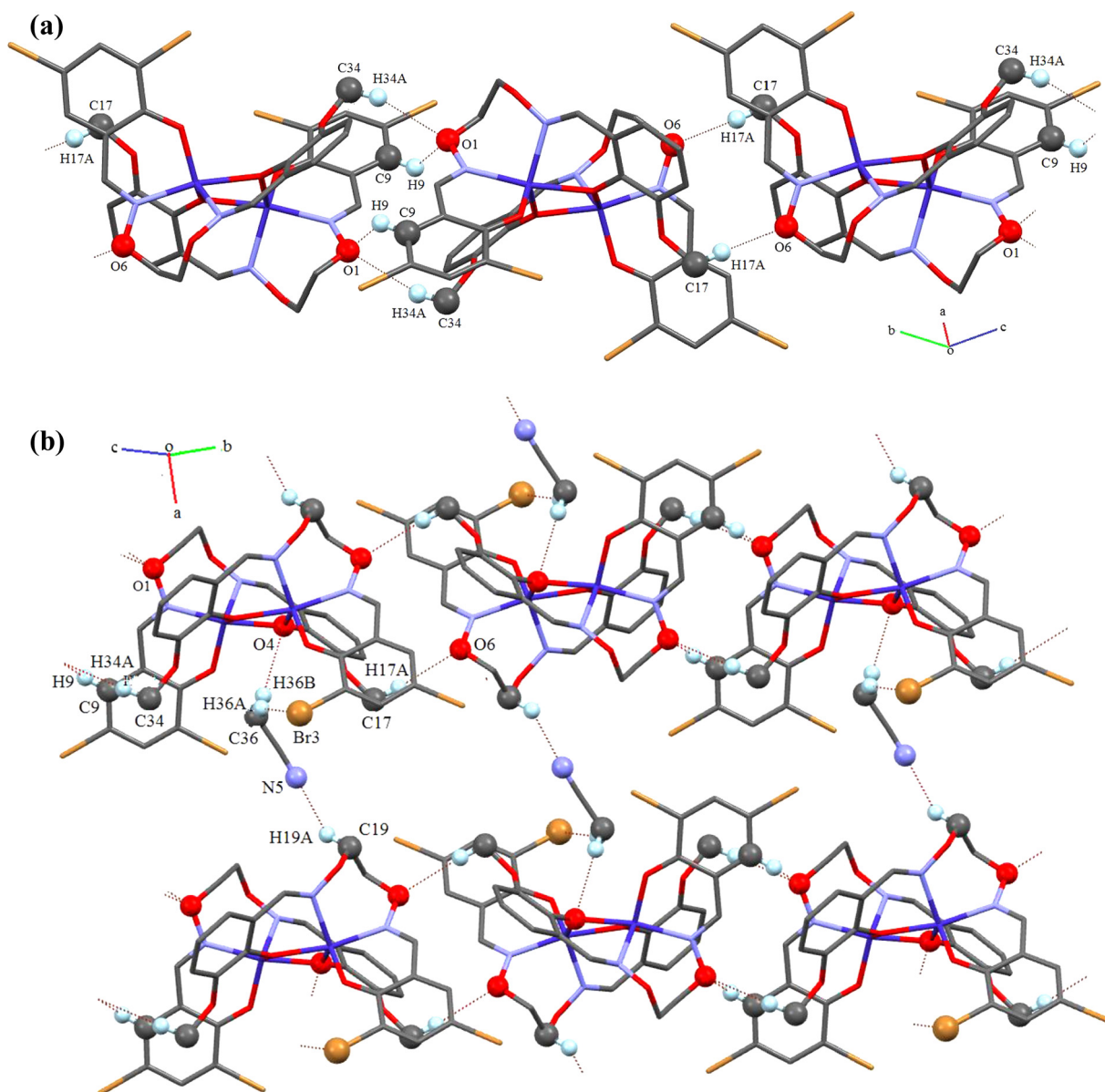


**Fig. 6.** Supramolecule structures of complex **3**. (a) View of the 1D chain motif within complex **3** along the *c* axis; (b) Part of 2D supramolecular layered structure via intermolecular and intramolecular hydrogen bond interactions.

**Table 4**

The most important FT-IR bands for the ligands and complexes **1**, **2** and **3** ( $\text{cm}^{-1}$ ).

| Compound  | $\nu_{(\text{C}=\text{N})}$ | $\nu_{(\text{Ar}-\text{O})}$ | Ph ring (C–H) | $\nu_{\text{O}-\text{H}}$ | $\delta_{(\text{H}-\text{O}-\text{H})}$ | $\rho_{\text{H}_2\text{O}}$ | $\nu_{(\text{M}-\text{O})}$ | $\nu_{(\text{M}-\text{N})}$ |
|---|-----------------------------|------------------------------|---------------|---------------------------|---|-----------------------------|-----------------------------|-----------------------------|
| $\text{H}_3\text{L}^1$                                    | 1614s                       | 1265s                        | 1480          | 3408w                     |   |                             |                             |                             |
| $[\text{Cu}(\text{HL}^1)]$                                | 1605s                       | 1203m                        | 1435vs        | 3420w                     |   |                             | 511w                        | 439w                        |
| $\text{H}_2\text{L}^2$                                    | 162s                        | 1246m                        | 1438vs        | 3408w                     |   |                             |                             |                             |
| $[\text{Cu}(\text{L}^2)\text{H}_2\text{O}]$               | 1601s                       | 1230m                        | 1476vs        | 3415s                     | 1636                                    | 547                         | 495w                        | 423w                        |
| $[\text{Co}_2(\text{L}^2)_2] \cdot 3\text{CH}_3\text{CN}$ | 1607s                       | 1244m                        | 1454vs        | 2926s                     |   |                             | 489w                        | 446w                        |

and **3**, respectively, and assigned to  $\text{L} \rightarrow \text{M}$  charge-transfer (LMCT) transitions which are characteristic of the transition metal complexes with  $\text{N}_2\text{O}_2$  coordination sphere [63].

#### 3.4. Fluorescence properties

The fluorescent properties of  $\text{H}_3\text{L}^1$  and its corresponding complex **1** were investigated at room temperature (Fig. 8a). The ligand  $\text{H}_3\text{L}^1$  exhibits an intense emission peak at 416 nm upon excitation

at 273 nm, which should be assigned to the intraligand  $\pi-\pi^*$  transition [64]. The Cu(II) complex **1** shows an intense broad photoluminescence with maximum emission at 462 nm upon excitation at 351 nm, which is slightly red-shifted by 46 nm compared to that of the ligand  $\text{H}_3\text{L}^1$ .

The emission spectra of  $\text{H}_2\text{L}^2$  and its corresponding complex **2** are shown in Fig. 8b. In comparison with the corresponding  $\text{H}_2\text{L}^2$  with the maximum emission wavelength at 417 nm when excited with 290 nm, the complex **2** exhibits red-shift with the maximum

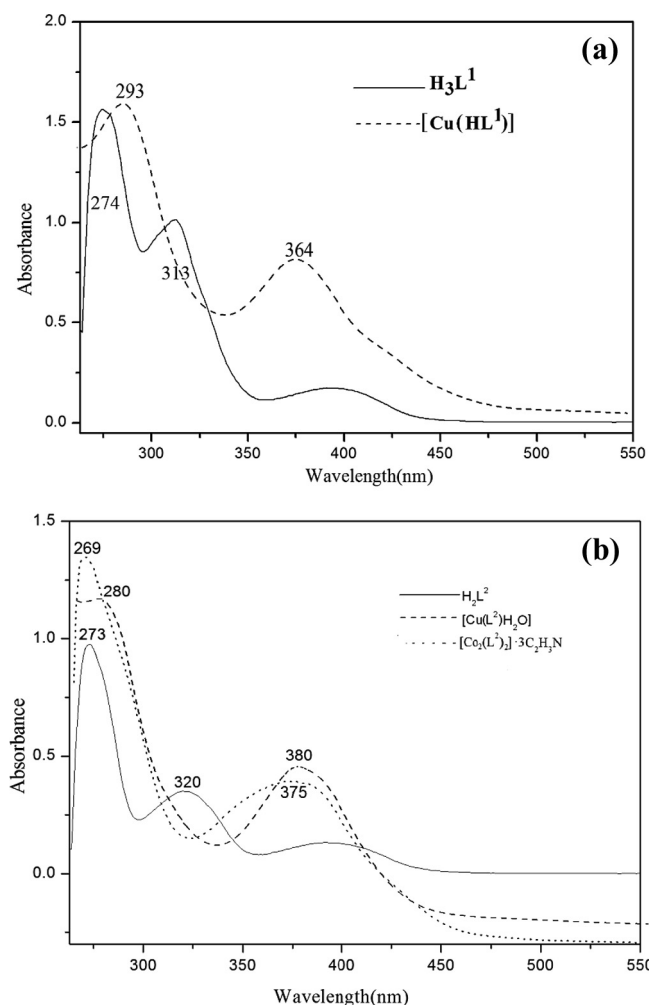


**Fig. 7.** UV-Vis absorption spectra of the ligands and their corresponding complexes. (a)  $H_3L^1$  (—) and its Cu(II) complex **1** (---) in DMF ( $5 \times 10^{-5} \text{ L}^{-1}$ ); (b)  $H_2L^2$  (—) and its Cu(II) (---) and Co(II) (-----) complexes **2** and **3**, respectively, in DMF ( $5 \times 10^{-5} \text{ mol L}^{-1}$ ).

emission wavelength  $\lambda_{\text{max}} = 473 \text{ nm}$  when excited at  $354 \text{ nm}$ , which could be assigned to the LMCT [65].

The blue emissions for complexes **1** and **2** have been observed. These complexes, having the same molar concentrations as the ligands, display enhanced emission intensities compared to their corresponding ligands  $H_3L^1$  and  $H_2L^2$  when excited with the similar amount of energy. Fluorescence enhancements through complexation are of much interest as it opens up the opportunity for photochemical applications of these complexes. The fluorescence of the free ligands  $H_3L^1$  and  $H_2L^2$  are probably quenched by the occurrence of a photoinduced electron transfer (PET) process due to the presence of a lone pair of nitrogen atoms. As such, the process is prevented by the complexation of the ligands  $H_3L^1$  and  $H_2L^2$  with Cu(II) atoms. Thus, the fluorescence intensities may be effectively enhanced by the coordination of Cu(II) atoms. Meanwhile, the chelation of the ligands  $H_3L^1$  and  $H_2L^2$  to Cu(II) atoms increases the rigidity of the ligands and therefore reduces the loss of energy via vibrational motions, which might increase the emission efficiency.

#### 4. Conclusions

According to the above data and discussion, three new supramolecular Cu(II) and Co(II) complexes with the chemical

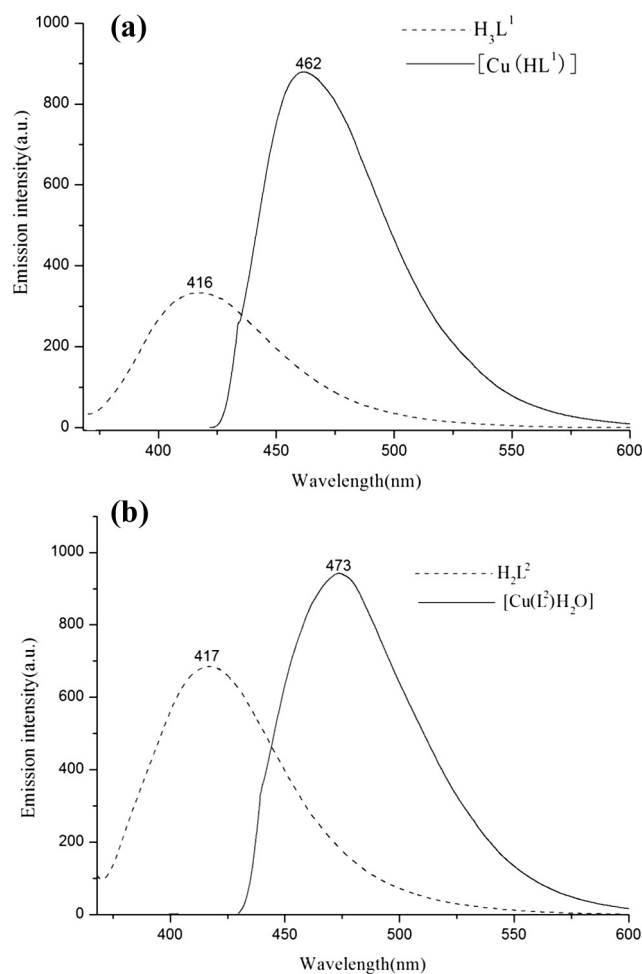


**Fig. 8.** Emission spectra of the ligands and their corresponding complexes. (a)  $H_3L^1$  (---) and its Cu(II) complex (—) in DMF ( $C = 5 \times 10^{-5} \text{ mol/L}$ ,  $\lambda_{\text{ex}} = 273$  and  $351 \text{ nm}$ ,  $\lambda_{\text{em}} = 416$  and  $462 \text{ nm}$ ); (b)  $H_2L^2$  (---) and its Cu(II) complex (—) in DMF ( $C = 5 \times 10^{-5} \text{ mol L}^{-1}$ ,  $\lambda_{\text{ex}} = 290$  and  $354 \text{ nm}$ ,  $\lambda_{\text{em}} = 417$  and  $473 \text{ nm}$ ).

formula  $[Cu(HL^1)]$  (**1**),  $[Cu(L^2)H_2O]$  (**2**) and  $[Co_2(L^2)_2] \cdot 3CH_3CN$  (**3**) with asymmetric Salamo-type ligands  $H_3L^1$  and  $H_2L^2$ , were synthesized and structurally characterized. In FT-IR spectra of complexes **1**, **2** and **3**, the  $\nu_{M-O}$  and  $\nu_{M-N}$  vibrational absorption frequencies have been observed. Meanwhile, the Cu(II) in complexes **1** and **2** exhibit blue emission with the maximum emission wavelengths at  $462$  and  $473 \text{ nm}$ , respectively. The structures of complexes **1**, **2** and **3** have serious distortion probably as a result of the introduction of different substituents into the two benzene rings of the asymmetric Salamo-type ligands.

#### Acknowledgements

This work was supported by the National Natural Science Foundation of China (21361015), Graduate Student Guidance Team Building Fund of Lanzhou Jiaotong University (260001) and the Science and Technology support funds of Lanzhou Jiaotong University (ZC2012003), which are gratefully acknowledged.

#### Appendix A. Supplementary data

CCDC 1433366, 1433367, and 1433368 contains the supplementary crystallographic data for **1–3**. These data can be obtained free of charge via <http://www.ccdc.cam.ac.uk/conts/retrieving.html>, or from the Cambridge Crystallographic Data Centre, 12

Union Road, Cambridge CB2 1EZ, UK; fax: (+44) 1223-336-033; or e-mail: deposit@ccdc.cam.ac.uk.

## References

- [1] H.L. Wu, H. Wang, X.L. Wang, G.L. Pan, F.R. Shi, Y.H. Zhang, Y.C. Bai, J. Kong, *New J. Chem.* 38 (2014) 1052.
- [2] H.L. Wu, Y.C. Bai, Y.H. Zhang, Z. Li, M.C. Wu, C.Y. Chen, J.W. Zhang, *J. Coord. Chem.* 67 (2014) 3054.
- [3] H.L. Wu, G.L. Pan, Y.C. Bai, Y.H. Zhang, H. Wang, F.R. Shi, X.L. Wang, J. Kong, *J. Photochem. Photobiol. B* 135 (2014) 33.
- [4] H.L. Wu, Y.C. Bai, Y.H. Zhang, G.L. Pan, J. Kong, F.R. Shi, X.L. Wang, *Z. Anorg. Allg. Chem.* 640 (2014) 2062.
- [5] T.Z. Yu, K. Zhang, Y.L. Zhao, C.H. Yang, H. Zhang, L. Qian, D.W. Fan, W.K. Dong, L. L. Chen, Y.Q. Qiu, *Inorg. Chim. Acta* 361 (2008) 233.
- [6] X.Q. Song, P.P. Liu, Z.R. Xiao, X. Li, Y.A. Liu, *Inorg. Chim. Acta* 438 (2015) 232.
- [7] P.P. Liu, L. Sheng, X.Q. Song, W.Y. Xu, Y.A. Liu, *Inorg. Chim. Acta* 434 (2015) 252.
- [8] X.Q. Song, Y.J. Peng, G.Q. Chen, X.R. Wang, P.P. Liu, W.Y. Xu, *Inorg. Chim. Acta* 427 (2015) 13.
- [9] J.C. Ma, X.Y. Dong, W.K. Dong, Y. Zhang, L.C. Zhu, J.T. Zhang, *J. Coord. Chem.* 69 (2016) 149.
- [10] R.H. Holm, E.I. Solomon, A. Majumdar, A. Tenderholt, *Coord. Chem. Rev.* 255 (2011) 993.
- [11] P. Chaudhuri, M. Hess, T. Weyhermüller, K. Wieghardt, *Angew. Chem., Int. Ed.* 38 (1999) 1095.
- [12] L.J. Klein, K.S. Alleman, D.G. Peters, J.A. Karty, J.P. Reilly, *J. Electroanal. Chem.* 481 (2000) 24.
- [13] H.L. Wu, G.L. Pan, Y.C. Bai, H. Wang, J. Kong, F.R. Shi, Y.H. Zhang, X.L. Wang, *Res. Chem. Intermed.* 41 (2015) 3375.
- [14] T. Storr, P. Verma, Y. Shimazaki, E.C. Wasinger, T.D.P. Stack, *Chem. Eur. J.* 16 (2010) 8980.
- [15] L. Wang, J.C. Ma, W.K. Dong, L.C. Zhu, Y. Zhang, *Z. Anorg. Allg. Chem.* 642 (2016) 834.
- [16] L.Q. Chai, G. Wang, Y.X. Sun, W.K. Dong, L. Zhao, X.H. Gao, *J. Coord. Chem.* 65 (2012) 1621.
- [17] P. Wang, L. Zhao, *Synth. React. Inorg. Met. Org. Nano Met. Chem.* 46 (2016) 1095.
- [18] Y.X. Sun, L. Wang, X.Y. Dong, Z.L. Ren, W.S. Meng, *Synth. React. Inorg. Met. Org. Nano Met. Chem.* 43 (2013) 599.
- [19] V.C. Gibson, S.K. Spitzmesser, *Chem. Rev.* 103 (2003) 283.
- [20] L. Rigamonti, F. Demartin, A. Forni, S. Righetto, A. Pasini, *Inorg. Chem.* 45 (2006) 10976.
- [21] Y.X. Sun, W.K. Dong, L. Wang, L. Zhao, Y.H. Yang, *Chin. J. Inorg. Chem.* 25 (2009) 1478.
- [22] X.Y. Dong, Y.X. Sun, L. Wang, L. Li, *J. Chem. Res.* 36 (2012) 387.
- [23] L. Zhao, L. Wang, Y.X. Sun, W.K. Dong, X.L. Tang, X.H. Gao, *Synth. React. Inorg. Met. Org. Nano Met. Chem.* 42 (2012) 1303.
- [24] L. Zhao, X.T. Dang, Q. Chen, J.X. Zhao, L. Wang, *Synth. React. Inorg. Met. Org. Nano Met. Chem.* 43 (2013) 1241.
- [25] P. Wang, L. Zhao, *Spectrochim. Acta, Part A* 135 (2015) 342.
- [26] H.L. Wu, C.P. Wang, F. Wang, H.P. Peng, H. Zhang, Y.C. Bai, *J. Chin. Chem. Soc.* 1028 (2015).
- [27] L. Xu, L.C. Zhu, J.C. Ma, Y. Zhang, J. Zhang, W.K. Dong, *Z. Anorg. Allg. Chem.* 641 (2015) 2520.
- [28] H.L. Wu, G.L. Pan, Y.C. Bai, H. Wang, J. Kong, F.R. Shi, Y.H. Zhang, X.L. Wang, *J. Chem. Res.* 38 (2014) 211.
- [29] V.T. Kasumov, F. Köksal, *Spectrochim. Acta, Part A* 61 (2005) 225.
- [30] S. Akine, F. Utsuno, T. Taniguchi, T. Nabeshima, *Eur. J. Inorg. Chem.* (2010) 3143.
- [31] L. Xu, Y.P. Zhang, J.Y. Shi, W.K. Dong, *Chin. J. Inorg. Chem.* 23 (2007) 1999.
- [32] L. Xu, Y.P. Zhang, L. Wang, J.Y. Shi, W.K. Dong, *Chin. J. Struct. Chem.* 27 (2008) 183.
- [33] Y.X. Sun, S.T. Zhang, Z.L. Ren, X.Y. Dong, L. Wang, *Synth. React. Inorg. Met. Org. Nano Met. Chem.* 43 (2013) 995.
- [34] Y.X. Sun, X.H. Gao, *Synth. React. Inorg. Met. Org. Nano Met. Chem.* 41 (2011) 973.
- [35] Y.X. Sun, L. Xu, T.H. Zhao, S.H. Liu, G.H. Liu, X.T. Dong, *Synth. React. Inorg. Met. Org. Nano Met. Chem.* 43 (2013) 509.
- [36] S. Akine, Z. Varadi, T. Nabeshima, *Eur. J. Inorg. Chem.* (2013) 5987.
- [37] W.K. Dong, F. Zhang, N. Li, L. Xu, Y. Zhang, J. Zhang, L.C. Zhu, *Z. Anorg. Allg. Chem.* 642 (2016) 532.
- [38] S. Akine, T. Taniguchi, W.K. Dong, S. Masubuchi, T. Nabeshima, *J. Org. Chem.* 70 (2005) 1704.
- [39] G.J. Kim, J.H. Shin, *Catal. Lett.* 63 (1999) 83.
- [40] W.K. Dong, J.C. Ma, L.C. Zhu, Y.X. Sun, S.F. Akogun, Y. Zhang, *Cryst. Growth Des.* 16 (2016) 6903.
- [41] W.K. Dong, S.J. Xing, Y.X. Sun, L. Zhao, L.Q. Chai, X.H. Gao, *J. Coord. Chem.* 65 (2012) 1212.
- [42] S. Akine, T. Taniguchi, T. Nabeshima, *Chem. Lett.* (2001) 682.
- [43] L.D. Jr, S.Y. Que, D. VanDerveer, X.R. Bu, *Inorg. Chim. Acta* 359 (2006) 197.
- [44] W.K. Dong, C.Y. Zhao, Y.X. Sun, X.L. Tang, X.N. He, *Inorg. Chem. Commun.* 12 (2009) 234.
- [45] W.K. Dong, J.G. Duan, Y.H. Guan, J.Y. Shi, C.Y. Zhao, *Inorg. Chim. Acta* 362 (2009) 1129.
- [46] W.K. Dong, J.H. Feng, X.Q. Yang, *Synth. React. Inorg. Metal Org. Nano Metal Chem.* 37 (2007) 189.
- [47] S. Akine, A. Akimoto, T. Shiga, H. Oshio, T. Nabeshima, *Inorg. Chem.* 47 (2008) 875.
- [48] W.K. Dong, X.N. He, H.B. Yan, Z.W. Lv, X. Chen, C.Y. Zhao, X.L. Tang, *Polyhedron* 28 (2009) 1419.
- [49] H.E. Smith, *Chem. Rev.* 83 (1983) 359.
- [50] M.G.B. Drew, R.N. Prasad, R.P. Sharma, *Acta Crystallogr., Sect. C* 41 (1985) 1755.
- [51] R.G. Xiong, B.L. Song, J.L. Zuo, X.Z. You, X.Y. Huang, *Polyhedron* 15 (1996) 903.
- [52] H.H. Yao, J.M. Lo, B.H. Chen, T.H. Lu, *Acta Crystallogr., Sect. C* 53 (1997) 1012.
- [53] W.K. Dong, Y.X. Sun, Y.P. Zhang, L. Li, X.N. He, X.L. Tang, *Inorg. Chim. Acta* 362 (2009) 117.
- [54] W.K. Dong, C.E. Zhu, H.L. Wu, T.Z. Yu, Y.J. Ding, *Synth. React. Inorg. Met. Org. Nano Met. Chem.* 37 (2007) 61.
- [55] S. Akine, *J. Incl. Phenom. Macrocyclic Chem.* 72 (2012) 25.
- [56] W.K. Dong, X. Li, C.J. Yang, M.M. Zhao, G. Li, X.Y. Dong, *Chin. J. Inorg. Chem.* 30 (2014) 1911.
- [57] W.K. Dong, Y.X. Sun, C.Y. Zhao, X.Y. Dong, L. Xu, *Polyhedron* 29 (2010) 2087.
- [58] W.K. Dong, G. Li, Z.K. Wang, X.Y. Dong, *Spectrochim. Acta, Part A* 133 (2014) 340.
- [59] M.M. Bhadbhade, D. Srinivas, *Inorg. Chem.* 32 (1993) 6122.
- [60] A. Panja, N. Shaikh, P. Vojtišek, S. Gao, P. Banerjee, *New J. Chem.* 26 (2002) 1025.
- [61] G.C. Percy, J. Thornton, *J. Inorg. Nucl. Chem.* 35 (1973) 2319.
- [62] S. Akine, Y. Morita, F. Utsuno, T. Nabeshima, *Inorg. Chem.* 48 (2009) 10670.
- [63] L. Gomes, E. Pereira, B. Castro de, *J. Chem. Soc., Dalton Trans.* (2000) 1373.
- [64] C.Y. Guo, Y.Y. Wang, K.Z. Xu, H.L. Zhu, Q.Z. Shi, S.M. Peng, *Polyhedron* 27 (2008) 3529.
- [65] R.J. Eglinski, S. Morris, D.E. Stevenson, *Polyhedron* 21 (2002) 2167.